ResearchGate

See discussions, stats, and author profiles for this publication at: https://www.researchgate.net/publication/256326056

An In Situ Spectroscopic Study of Prochiral Reactant−Chiral Modifier Interactions on Palladium Catalyst: Case of Alkenoic Acid and Cinchonidine in Various Solvents

ARTICLE *in* THE JOURNAL OF PHYSICAL CHEMISTRY C · JULY 2013

Impact Factor: 4.77 · DOI: 10.1021/jp403273c

CITATIONS
9

READS
38

2 AUTHORS:

Shuai Tan
Georgia Institute of Technology
14 PUBLICATIONS **28** CITATIONS
SEE PROFILE

Christopher T Williams
University of South Carolina
132 PUBLICATIONS **2,114** CITATIONS
SEE PROFILE

Available from: Shuai Tan
Retrieved on: 17 January 2016

THE JOURNAL OF PHYSICAL CHEMISTRY C

Article

pubs.acs.org/JPCC

An In Situ Spectroscopic Study of Prochiral Reactant−Chiral Modifier Interactions on Palladium Catalyst: Case of Alkenoic Acid and Cinchonidine in Various Solvents

Shuai Tan and Christopher T. Williams*

Department of Chemical Engineering, University of South Carolina, Columbia, South Carolina 29208, United States

Supporting Information

ABSTRACT: In situ attenuated total reflection infrared (ATR-IR) spectroscopy has been used to study the adsorption of a model α,β-unsaturated carboxylic acid (2-methyl-2-pentenoic acid) and chiral modifier (cinchonidine), as well as their intermolecular interactions, on Pd/Al_2O_3 in typical polar (methanol) and nonpolar (dichloromethane) solvents. It has been found that the solvent has essentially no effect on cinchonidine adsorption. The carboxylic acid tends to adsorb on surface through bridging bidentate carboxylate in MeOH instead of monomer or dimer species, which is prevalent in the case of CH_2Cl_2. Moreover, an acid−cinchonidine complex prefers to form in a substrate to modifier ratio of 1:1, regardless of whether it is in the bulk solution or adsorbed on the surface. Thus, direct spectroscopic observation of an important intermediate in this catalytic system has been made.

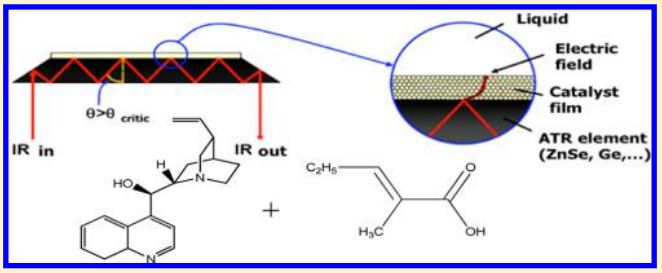

INTRODUCTION

Asymmetric hydrogenation has proved to be a promising method for chiral molecules produced in industrial applications, such as for pharmaceuticals and agrochemicals.[1,2] Significant success has been achieved by homogeneous catalysis.[3,4] However, only limited asymmetric synthesis reactions have been approached commercially in the field of heterogeneous catalysis, including C═O bond hydrogenation of prochiral ketones and ketoesters over tartaric acid modified Ni[5−7] or cinchona alkaloid modified Pt.[8−10] It has been found that the cinchona alkaloid modified Pd catalyst is more effective than Ni or Pt for C═C bond hydrogenation of unsaturated carboxylic acids, including alkenoic acids,[11−15] although the studies of this type of reaction are much less than in the two previous cases.

It has been revealed by both theoretical modeling[16,17] and experimental studies[18−21] that cinchona alkaloids exhibit a very rich conformational behavior, which is the key for leading to a preferential formation of an enantiomer. In general, the orientation of quinoclidine N atom (i.e., points away/toward the quinoline ring) is the central role in controlling this behavior. Initially, several UHV-based techniques were applied in the study of adsorption of cinchona alkaloid on metal surface. For instance, the adsorption of 10,11-dihydrocinchonidine (DHC) on Pt(111) was studied by use of X-ray photoelectron spectroscopy (XPS) and low-energy electron diffraction (LEED).[22,23] Along with mass spectroscopy (MS) and H-D isotope exchange experiments,[24,25] these measurements confirmed that the quinoline moiety of the molecule is lying parallel to the metal surface through a π-electron interaction at room temperature, and becomes tilted at 323K,[26] although these UHV-based experiments were far from the real reaction condition.

Through the end of the last century, there was no information regarding the surface of chiral-modified metals under conditions approaching those of the actual reaction conditions (i.e., liquid phase, elevated H_2 pressures). The application of in situ vibrational spectroscopic techniques such as infrared reflection−absorption spectroscopy (IRAS)[27,28] and attenuated total reflection infrared (ATR-IR) spectroscopy[29−33] has made it possible to begin to address this situation over the past decade and moving forward.

A more important issue in the enantioselective hydrogenation of alkenoic acid other than simple adsorption behavior of the modifier and the substrate is the investigation of intermolecular interactions, which is crucial for catalytic performance in terms of activity and enantioselectivity. A deeper investigation of these aspects needs to be studied in order to further understand and optimize such catalytic systems. Compared to the well-known ketone/ketoester−cinchonidine−Pt system,[34−36] studies of the alkenoic acid−cinchonidine−Pd system are limited under conditions[37] that represent the actual chemical environment encountered during hydrogenation. Therefore, in this paper the in situ ATR-IR technique is applied to examine of adsorption of alkenoic acid and cinchonidine, along with their intermolecular interactions at the Pd surface.

Received: April 2, 2013
Revised: July 21, 2013

 © XXXX American Chemical Society dx.doi.org/10.1021/jp403273c | J. Phys. Chem. C XXXX, XXX, XXX−XXX

EXPERIMENTAL SECTION

Materials. Cinchonidine (CD, 98.0%, Fluka, Figure 1), *trans*-2-methyl-2-pentenoic acid (MPeA, 98%, SAFC, Figure 1),

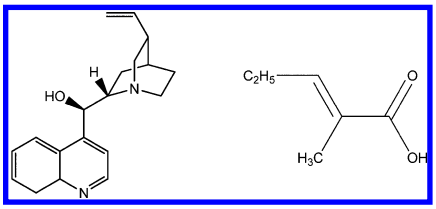

Figure 1. Structure of cinchonidine (CD, left) and *trans*-2-methyl-2-pentenoic acid (MPeA, right).

dichloromethane (99.9%, Sigma-Aldrich), methanol (99.9%, Alfa-Aesar), 5 wt % Pd/γ-Al_2O_3 powder (Alfa-Aesar), γ-Al_2O_3 powder (45 m^2/g, 37 nm, Alfa-Aesar), and 0.3 and 0.05 μm alumina suspension (Allied High Tech Products) were used as received. Deionized water with 18.2 MΩ was obtained by using a Barnstead water system with nanopure and B-pure filter.

Film Preparation. Before film preparation, the ZnSe internal reflection element (IRE) was cleaned with a polishing cloth in 0.3 and 0.05 μm alumina suspensions and flushed with deionized water. The thin film of support or catalyst powder was deposited on the ZnSe element for ATR-IR spectroscopic study. To be specific, ca. 50 mg of Al_2O_3 or Pd/Al_2O_3 powder was mixed with 20 mL of DI water in a glass bottle to form a suspension. The suspension was placed into an ultrasonic bath to sonicate overnight to decrease any agglomeration in solution. To deposit a film, the suspension was sucked by pipet and dropped onto a 70 × 10 × 3 mm ZnSe IRE (Spectral Systems, 60 degree) and dried out at room temperature.[32] In summary, the film exhibits satisfactory properties in terms of thickness (ca. 3−4 times larger than ATR-IR penetration depth) and stability (more than 24 h in the presence of flowing solvent). The void fraction is a parameter that should be mentioned since this value reflects the possible signal contribution due to the liquid phase filled in this space. Such factor has been investigated in the previous study of the author's group.[38] In short, since the Al_2O_3 particles are quite uniform in size, it is reasonable to expect that the fraction has a number of ca. 0.26 assuming a close-packed geometry arrangement.

In Situ ATR-IR Spectroscopy. A flowchart of the ATR-IR system is depicted in Figure 2 with an insertion of the detailed view of flow cell accessories. The mixture solution and pure solvent were stored in separate reservoirs with magnetic stirrers. A homemade brass flow cell sealed with O-ring, having a 1.1 cm^3 channel for liquid flow over the coated IRE surface, was used with an ATR accessory from Thermo Nicolet. The liquid flow rates were set to 20−25 mL/min. All tubes were made of Teflon due to its chemical resistance to solvent, acid, and cinchonidine. By switching the valves, the system can control the type of liquid that flows through the cell. The entire system is managed by Labview software.

The coated ZnSe IRE was mounted in the flow cell and maintained to room temperature (20 °C) during the entire experiment. Purging the IRE with solvent for at least 4 h before starting experiment was found to be necessary to remove the surface contaminants and any loose powder and reach a stable FT-IR signal. The in situ ATR-IR spectra of the solid−liquid interface were recorded with a Nicolet 670 infrared spectrometer equipped with a liquid nitrogen-cooled MCT detector. A spectrum of pure solvent was collected as the background for the samples measured on bare element. In contrast, for the case of thin film samples, the background was taken in the presence of the film and pure solvent after the system had stabilized. Each spectrum was acquired using 4 cm^{-1} resolution and 96 scans.

RESULTS AND DISCUSSION

Single-Component Adsorption. Prior to the ATR-IR studies of substrate−modifier interaction, the spectra of both components at different surfaces were first investigated. Figure 3 shows the ATR-IR spectra of MPeA solution (16 mM) and

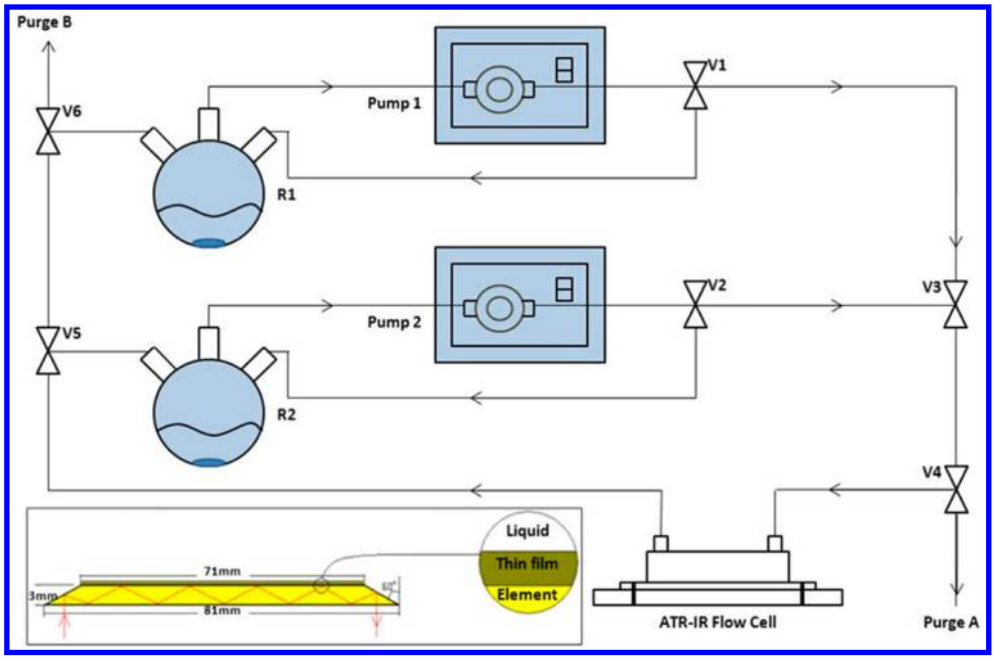

Figure 2. Schematic of the ATR-IR flow system with side view of flow cell and accessories.

dx.doi.org/10.1021/jp403273c | J. Phys. Chem. C XXXX, XXX, XXX−XXX

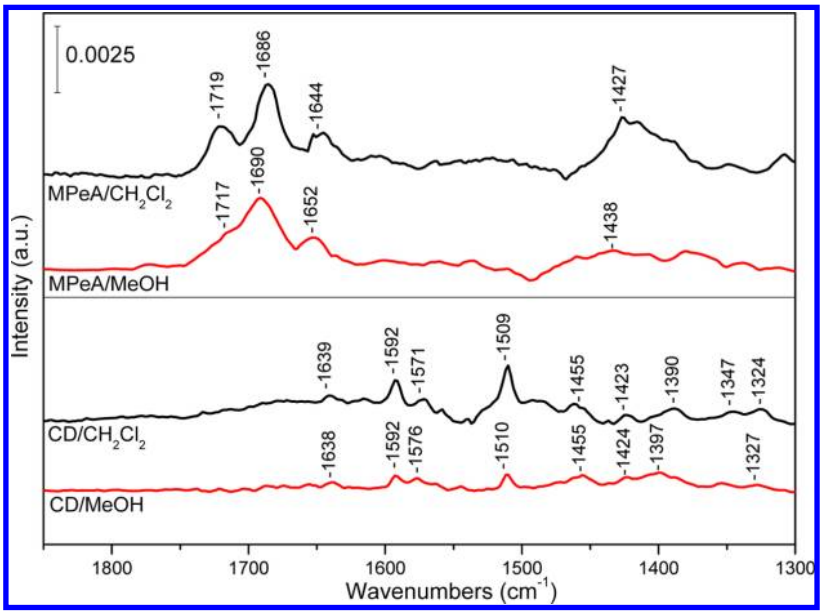

Figure 3. ATR-IR spectra of MPeA (16 mM) and CD (10 mM) in CH_2Cl_2 and MeOH solutions on bare element.

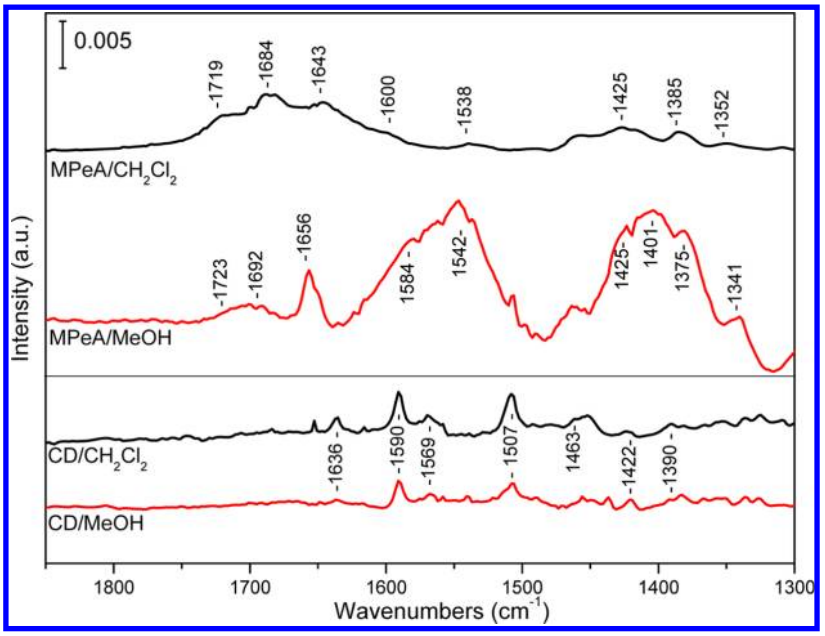

Figure 4. ATR-IR spectra of MPeA (16 mM) and CD (10 mM) in CH_2Cl_2 and MeOH solutions on γ-Al_2O_3 surface.

CD solution (10 mM) on bare element with CH_2Cl_2 and MeOH as solvents. For the case of MPeA/CH_2Cl_2 mixture, the bands are assigned as ν(C═O) in monomer at 1719 cm^{-1}, while the dimeric ν(C═O) stretch appears at 1686 cm^{-1}. The 1644 and 1427 cm^{-1} features are due to ν(C═C) and δ(C−H), respectively, from these species. In MPeA/MeOH solution, the acid vibrational bands remain at the similar position, but with monomeric ν(C═O) becoming weaker.

It should be mentioned that curve-fitting methodology was applied for peak assignment of MPeA in solution and on surfaces. Initially, the individual peak parameters (i.e., position, full width at half-maximum (FWHM), and height) were chosen based on visual inspection of the experimental spectrum. Then the residual between the overall fit and raw spectrum was minimized by minimizing the square root of the sum of square errors in an iterative fashion. All the peaks were modeled by pure Gaussian line shapes. The detailed procedure of spectrum deconvolution of MPeA in solution and on various surfaces was explained in detail in our previous studies.[32,33] The specific process has again been outlined in the Supporting Information provided.

IR spectra of CD in bulk phase[39] and liquid phase[40] and as an adsorbate on metals such as Pt[29] and Pd[30] have been studied extensively. In this present work, the peak assignment of CD follows previous work from our group[39] and others.[41] The traces at the bottom of Figure 3 show the ATR-IR spectra from liquid CD solutions, with features observed at 1639, 1592, 1571, 1509, 1455, 1423, 1390, 1347, and 1324 cm^{-1} in CH_2Cl_2. It is also found that, for the case of MeOH, most of vibrational band positions have only 1−3 cm^{-1} difference, which is negligible given the resolution of the measurement.

dx.doi.org/10.1021/jp403273c | J. Phys. Chem. C XXXX, XXX, XXX−XXX

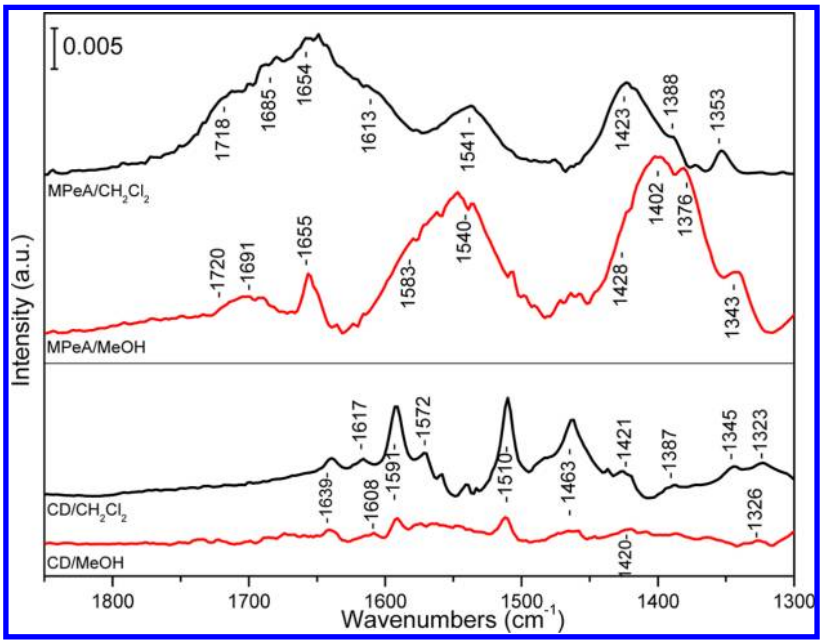

Figure 5. ATR-IR spectra of MPeA (16 mM) and CD (10 mM) in CH_2Cl_2 and MeOH solutions on Pd/γ-Al_2O_3 surface.

The adsorption of MPeA and CD on γ-Al_2O_3 surfaces was studied under the same concentration solutions followed by purging with pure solvent for 1 h. Figure 4 shows the spectra of adsorbed MPeA and CD on the Al_2O_3 surface. The bands for adsorbed MPeA in CH_2Cl_2 solution were deconvoluted and assigned in our previous work.[32] In short, the 1719 and 1684 cm^{-1} features are from the ν(C═O) stretches for monomer and dimer species, respectively. The 1643 cm^{-1} band is from the ν(C═C), while the shoulder at 1600 cm^{-1} along with 1538 cm^{-1} feature are both assigned as $\nu_{as}(COO^-)$. The feature at 1385 cm^{-1} is due to a $\nu_s(COO^-)$. In contrast, for the case of MeOH solvent, it is observed that the ν(C═O) stretches for both monomeric and dimeric species at ca. 1723 and 1692 cm^{-1} have greatly diminished. However, the ν(C═C) band at 1656 cm^{-1} sharpened, and $\nu_{as}(COO^-)$ stretches at 1584 and 1542 cm^{-1} have strengthened. The $\nu_s(COO^-)$ stretches at 1401 and 1375 cm^{-1} have also become stronger. This indicates that, with MeOH solvation, MPeA tends to more favorably form strongly adsorbed carboxylate on the Al_2O_3 surface, with less amount of molecular species, which is quite different from the case of CH_2Cl_2.

Moreover, it is noticed that both the $\nu_{as}(COO^-)$ and $\nu_s(COO^-)$ have a slightly red shift for ca. 10−20 cm^{-1}, in the presence of MeOH solvent. This is possibly due to H-bonding interaction between solvent molecule and solute. To be specific, the H atom in the hydroxyl group in MeOH interacts with O atom of carboxylate adsorbed at the surface. Therefore, the negative charge at $-COO^-$ could partly transfer, leading to a redistribution of electron density, which consequently affects the vibrational frequency.

In contrast to Burgi's study,[41] adsorption of CD on Al_2O_3 surface is observed here, as shown in the bottom of Figure 4. This observation is supported by Li and co-workers[42] who investigated the adsorption and decomposition of ethyl pyruvate (EtPy) over chiral-modified Pt/γ-Al_2O_3 by using ethanol as solvent. The main bands are observed at 1636, 1590, 1569, 1507, 1463, 1422, and 1390 cm^{-1}, which is similar to the case of bare element. Moreover, comparing the spectra of CD adsorption on Al_2O_3 in Figure 4, the similar band shapes and positions indicate that the solvent has little effect on CD adsorption.

Next, the spectra obtained during adsorption of MPeA and CD on Pd/Al_2O_3 were acquired and are summarized in Figure 5. Similar to the case of MPeA adsorption on Al_2O_3, the presence of MeOH as solvent dramatically affects the spectrum in terms of peak position and peak intensity. To be specific, the broadened peaks at 1500−1600 and 1350−1450 cm^{-1} regions indicate that MPeA tends to form carboxylate at the surface instead of molecular species in MeOH. Moreover, it should be mentioned that, in CH_2Cl_2 solvent, MPeA shows stronger band intensity at ca. 1541 and 1423 cm^{-1} in case of Pd/Al_2O_3 rather than only Al_2O_3. This indicates that the presence of Pd particles could increase the adsorption capacity with respect to the carboxylate.

The adsorption of CD in the two solvents shows very similar spectra, with strong signal in the 1500−1600 cm^{-1} region due to in-plane quinoline ring stretch. Considering Greenler's well-known IR selection rules,[43] the intensity of molecular vibrations parallel to metal surfaces will be greatly diminished (or not observed) due to cancellation from the image dipole effect. This suggests that a tilted orientation with respect to the Pd surface is favored under the current condition. This conclusion is consistent with Baiker's previous investigation, mentioning that peaks at 1586 and 1501 cm^{-1} are due to N lone pair bonded tilted species, while the band at 1567 cm^{-1} is due to π-bonded parallel species.[30] Interestingly, for CD adsorption, the peak intensities in CH_2Cl_2 are always larger than those in MeOH (see Figures 3, 4, and 5). According to Zaera and co-workers,[44] the solubility of CD in MeOH (73 g/L) is almost 6 times as much as in CH_2Cl_2 (12 g/L). Considering a solubility−adsorption correlation, the greater ATR-IR signal in CH_2Cl_2 is due to more surface-covered CD in this solvent. It also should be noted that, in CH_2Cl_2 solvent, the peak intensity of adsorbed CD in presence of Pd particles is much greater than in the case of just Al_2O_3. Given the low weight percent (5%) and metal surface area (<4 m^2 metal/$g_{catalyst}$) of Pd, this observation indicates that the CD is much more strongly

dx.doi.org/10.1021/jp403273c | J. Phys. Chem. C XXXX, XXX, XXX−XXX

adsorbed on the metal. The similar band intensity in the case of MeOH is again probably due to the high solubility of CD.

The list of peak assignments of MPeA and CD in solution and adsorbed on surfaces are provided in Tables 1 and 2,

Table 1. Peak Assignments of MPeA in the Liquid Phase and Adsorbed in MeOH and CH_2Cl_2

in solution MeOH (CH_2Cl_2[a])	on Al_2O_3 MeOH (CH_2Cl_2[a])	on Pd/Al_2O_3 MeOH (CH_2Cl_2[a])	assignment
1717 (1719)	/(1719)	/(1718)	C═O str (monomer)
1690 (1686)	/(1684)	/(1685)	C═O str (dimer)
1652 (1644)	1656 (1643)	1655 (1654)	C═C str
/	1584 (1600)	1583 (1613)	COO^- asym str
/	1542 (1538)	1540 (1541)	COO^- asym str
1438 (1427)	1425 (1425)	1428 (1423)	C−H def
/	1401 (/)	1402 (/)	COO^- sym str
/	1375 (1385)	1376 (1388)	COO^- sym str
1339 (1350)	1341 (1352)	1343 (1353)	C═C−H def

[a]Published in previous work.[32]

respectively. To summarize our ATR-IR studies of single-component adsorption, the presence of MeOH leads MPeA to preferentially form adsorbed carboxylate species, which strongly adsorb on the metal/oxide surface. This effect is probably due to H-bonding interactions, which are lacking in CH_2Cl_2. However, for the case of cinchonidine adsorption, the properties of solvents (i.e., polarity, H-bonding) do not significantly affect the adsorption geometry and orientation of adsorbate, although the band intensity varies due to different solubility.

Substrate−Modifier Interaction Study. Since the interaction between the acid and cinchonidine plays a key role in determining the acid−modifier complex structure and orientation with respect to the surface, ATR-IR was used to investigate this issue. In Figure 6, the CD concentration was fixed at 10 mM. The MPeA/CD ratio was adjusted by injecting MPeA into the reservoir, ranging from 0.5 to 2 equiv with respect to CD. It can be seen that, along with the increase in MPeA concentration, a growth in the spectral intensity appears in the regions of 1360−1410 and 1520−1560 cm^{-1}. As can be seen, altering the acid/modifier ratio does not affect either band position or shape, although the intensity varies. It is known that the peak at ca. 1390 cm^{-1} is due to the C_8-C_9 stretch of CD, where C_8 is the neighbor carbon atom of quinoclidine N atom, and C_9 is the chiral carbon atom of cinchonidine. The band at 1460 cm^{-1} is assigned as quinoclidine $-CH_2$ out-of-plane scissoring. However, the spectral envelope between 1520 and 1560 cm^{-1} does not belong to either MPeA or CD in CH_2Cl_2, indicating that they arise from a substrate−modifier interaction. The observations are supported by an FT-IR study of the CD−tiglic acid interaction in the liquid phase.[45]

Moreover, it is found that, up to a 1/1 MPeA/CD ratio, MPeA featured bands associated with dimer and monomers in solution are not observed. However, above this ratio, the expected bands (between 1670 and 1720 cm^{-1}) appear just as if acid were alone in solution. Such behavior suggests that the type of intermolecular interaction involves substrate with modifier in a 1:1 ratio. The complex prevents the acid from either forming a dimer or remaining in solution as a monomer species. Therefore, judging from the structure of CD and MPeA, such interaction is probably due to H-bonding between −OH group from CD and carbonyl group of the acid, as well as the easily-protonated N atom of the quinoclidine moiety of the CD and −OH groups of the acid. The current proposed 1:1 model has been supported by Vaccari's kinetic study of the tiglic acid−CD−Pd system, with the observation that dilution of reactant does not affect the enantiomeric excess (e.e.) value.[46] In fact, the disappearance of the C═O vibrational bands strongly suggests that the complex is a carboxylate salt formed between the CD and MPeA. Unfortunately, examination of the OH stretching region of the spectra revealed no clear trends, as the signal in this region was very noisy and was not very reproducible.

Next, the intermolecular interaction of the surface-adsorbed MPeA−CD complex was investigated. A spectrum of 16 mM MPeA/CH_2Cl_2 mixture flowing over the catalyst surface was first obtained and is shown in Figure 7. Then, CD was stepwise added into the liquid mixture to reach various CD/MPeA ratios

Table 2. Peak Assignments of Cinchonidine in the Solid Phase and Liquid Phase and as Adsorbate

	in solution		on Al_2O_3		on Pd/Al_2O_3		
solid	MeOH	CH_2Cl_2	MeOH	CH_2Cl_2	MeOH	CH_2Cl_2	assignment[a]
1635	1638	1639	1636	1636	1639	1639	C═C str
1617		1615		1617	1608	1617	Q ip def + QC-H ip bend
1591	1592	1592	1590	1590	1591	1591	Q ip def + QC-H ip bend
1568	1576	1571	1569	1569	1574	1572	Q ip def + QC-H ip bend
1508	1510	1509	1507	1507	1510	1510	Q ip def + QC-H ip bend
1462		1464	1463	1463	1463	1463	QN $C(7)H_2$ op scissor
1452	1455	1455		1451		1451	QN $C(5)H_2$ op scissor
1421	1424	1423	1422	1422	1420	1421	Q ip def
	1397	1390	1390	1390			C(8)−C(9) str
1383	1386		1385		1386	1387	Q str + CH ip bend
1367			1364		1363		Q str + CH ip bend
1358			1360				C═C−C def
1336		1347		1337		1345	Q str + QN C(8)H wag
1326	1327	1324		1326	1326	1323	QN CH_2 wag + Q ip def
1307							QN CH and CH_2 wag

[a]ip = in plane; op = out of plane; Q = quinoline ring; QN = quinuclidine.

dx.doi.org/10.1021/jp403273c | J. Phys. Chem. C XXXX, XXX, XXX−XXX

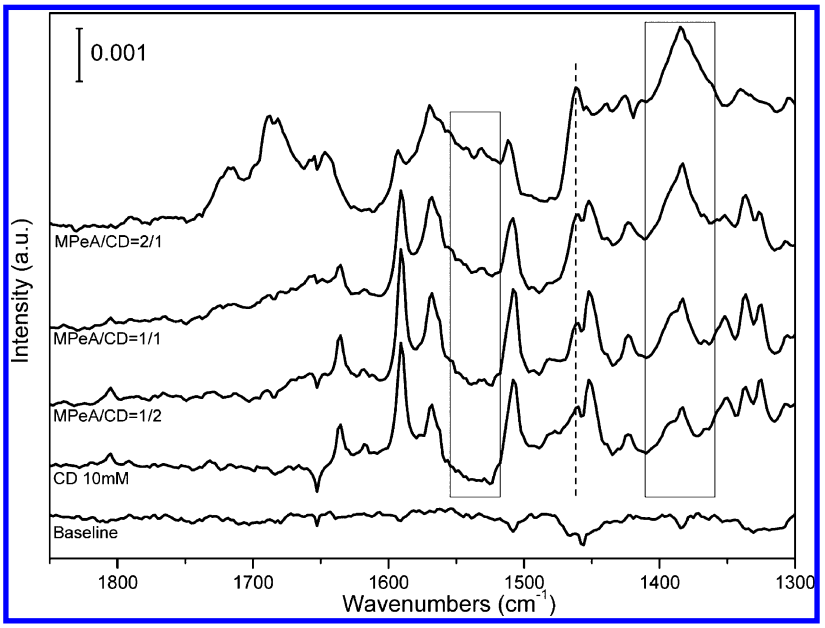

Figure 6. ATR-IR spectra of MPeA/CD at different ratios in CH_2Cl_2 solution on bare element.

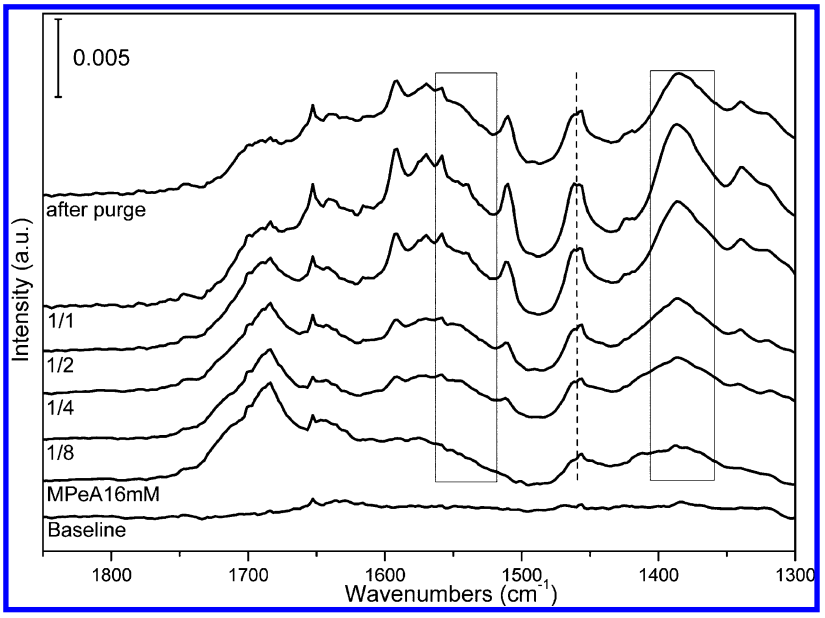

Figure 7. ATR-IR spectra of CD/MPeA at different ratios in CH_2Cl_2 solution on Pd/γ-Al_2O_3 surface.

from 1:8 to 1:1. Finally, to examine the contribution of liquid phase, the cell was flushed with pure solvent for 1 h until a steady signal was reached and a final spectrum was obtained (top spectrum, Figure 7). It is found that, after this purging, the peak intensity was slightly decreased due to the desorption of surface species and removal of liquid. As the CD concentration was increased, the MPeA-related bands in the 1650−1750 cm^{-1} region (ν(C═O) of both monomer and dimer) decreased in intensity. This suggests that the presence of CD prevents the substrate acid from staying as a molecular species. Meanwhile, even at the smallest ratio (1/8), the peaks belonging to the quinoline ring of CD (1515, 1570, and 1590 cm^{-1}) start to appear. Moreover, these peaks keep increasing with increased CD concentration. In addition, at 1460 cm^{-1} and in the 1360−1410 and 1520−1560 cm^{-1} regions, the band intensities increased with addition of CD, suggesting the formation of an intermolecular interaction at the Pd/Al_2O_3 surface. By comparing Figures 6 and 7, clearly the intermolecular interactions show up at same region, although the intensity differs. This suggests that the acid−modifier complex exhibits a specific type of interaction, regardless of the ratio of two species, and whether the complex exists in solution or adsorbed at the surface.

The same experiment was carried out in MeOH solvent. As can be seen in Figure 8, although the MPeA shows peaks in the region of 1360−1410 and 1520−1560 cm^{-1}, shoulders and bands at 1510, 1574, and 1590 cm^{-1} due to quinoline ring deformation of the modifier could be observed with increasing CD, indicating a replacement of adsorbed substrate acid by modifier.

Finally, it is interesting to determine if the adsorption sequence will affect this interaction. To examine this, a series of

dx.doi.org/10.1021/jp403273c | J. Phys. Chem. C XXXX, XXX, XXX−XXX

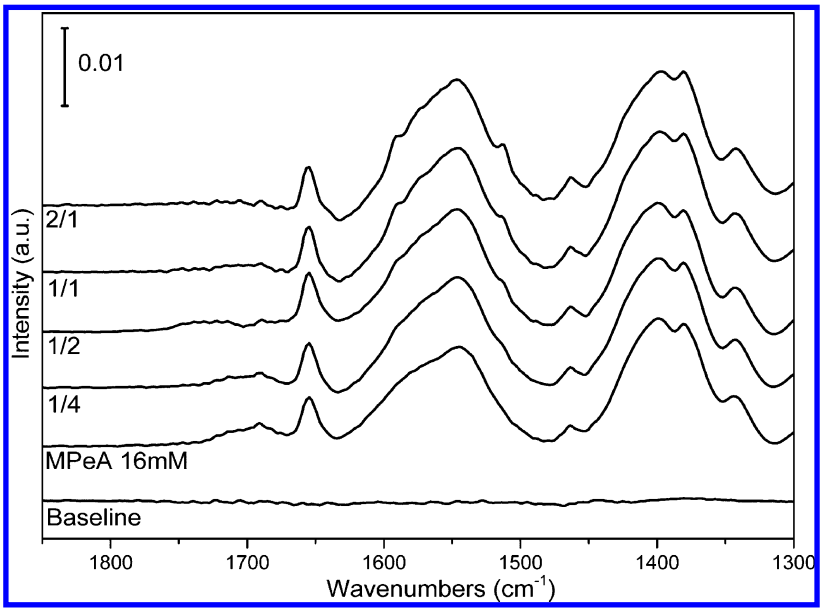

Figure 8. ATR-IR spectra of CD/MPeA at different ratios in MeOH solution on Pd/γ-Al_2O_3 surface.

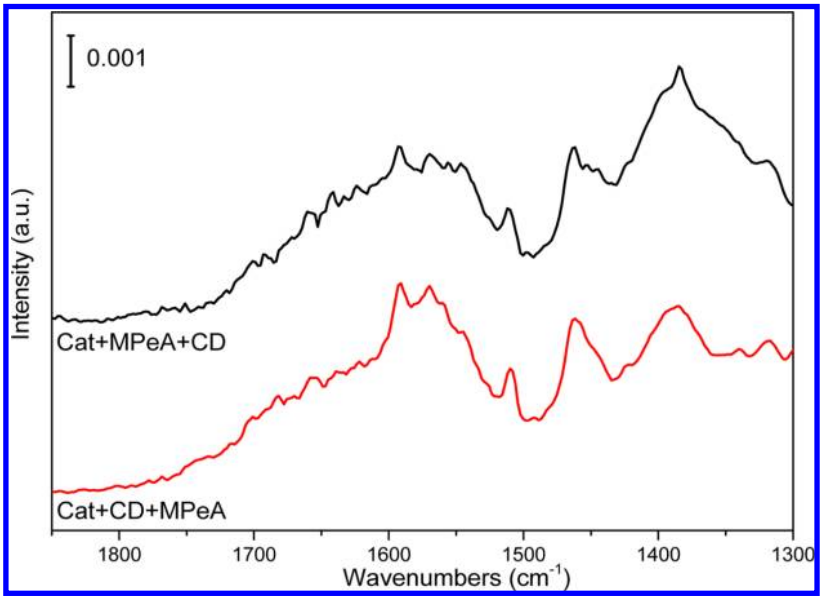

Figure 9. Sequential ATR-IR study of CD−MPeA interaction in CH_2Cl_2 solution on Pd/γ-Al_2O_3 surface.

experiments were carried out based on the following routine. The two species (20 mM substrate acid and 10 mM modifier) were introduced onto Pd/Al_2O_3 surface in sequential order with solvent flushing between the steps, followed by solvent purging. Approximately 50 mL of pure solvent was used in flushing the film for about 30 min. Then, the final obtained spectra were compared and are shown in Figures 9 and 10 for CH_2Cl_2 and MeOH, respectively. As can be seen, the spectral features at 1360−1410 and 1520−1560 cm^{-1} due to acid−modifier complex, although exhibiting slightly different intensity, show up at the same region, demonstrating again a specific type of intermolecular interaction regardless of the adsorption sequence of acid and modifier.

Thus, we propose a modifier−acid = 1:1 complex model under the current conditions. Previously, Nitta,[47] Bartok,[48−51] and Szollosi[52] have assumed this type of intermediate in polar solvent such as MeOH and DMF according to kinetic observations for both aliphatic and aromatic substrate, which is consistent with the current study. In contrast, Baiker, assuming that alkanoic acids prefer to form a dimer in apolar medium, suggested a 1:2 modifier:acid complex in nonpolar solvent. Their conclusion is based on the observation that no further increase of the e.e. value was achieved when CD/acid ratio varied from 0.5 to 1.[11] It has been pointed out that both quinoclidine N atom and C_9−OH, as well as the combination of C_8−C_9 configuration, are directly involved in the chiral recognition in such systems in a recent DFT calculation.[53] Since not many studies have been reported regarding the dependence of kinetic behavior on CD/acid ratio, determining the preferred complex structure from a kinetic standpoint requires further investigation. Nevertheless, the present study provides direct spectroscopic evidence of the active substrate−modifier complex at the metal surface under a liquid phase condition (although in the absence of dissolved hydrogen).

dx.doi.org/10.1021/jp403273c | J. Phys. Chem. C XXXX, XXX, XXX−XXX

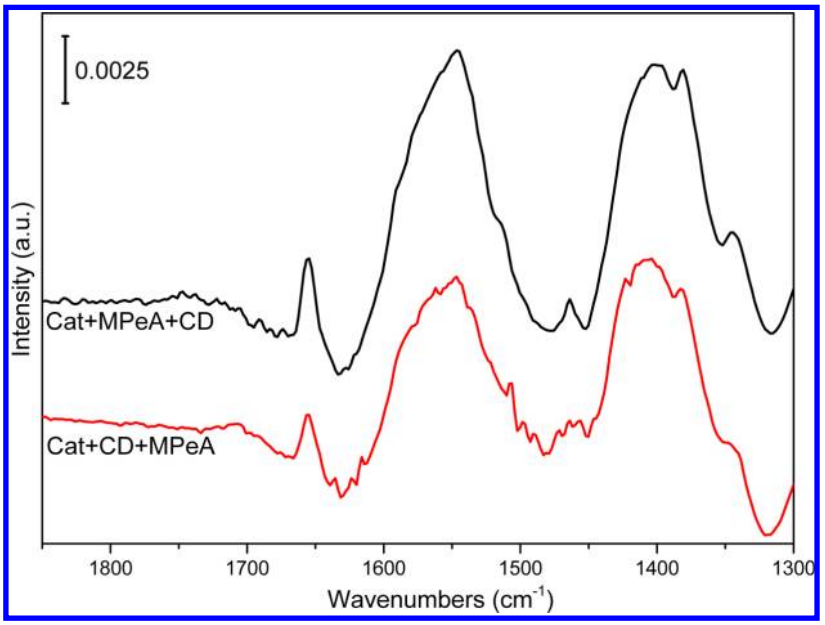

Figure 10. Sequential ATR-IR study of CD−MPeA interaction in MeOH solution on Pd/γ-Al_2O_3 surface.

Further studies are planned to directly correlate the presence of this species with kinetic behavior observed in batch studies.

CONCLUSION

In this paper, an adsorption study of MPeA and CD at Al_2O_3 and Pd/Al_2O_3 surfaces in two solvents (MeOH and CH_2Cl_2) with in situ ATR-IR technique was conducted. In the presence of MeOH solvent, the vibrations associated with adsorbed carboxylate exhibit a wavenumber shift, likely due to the H-bonding between solvent and acid molecule. However, the different solvents do not appear to affect the adsorption behavior of cinchonidine in terms of adsorption orientation. The fixed band position (1360−1410 and 1520−1560 cm^{-1}) and peak shape of the substrate−modifier complex in the investigation of intermolecular interaction demonstrates that the modifier shows a preferred adsorption on Pd/Al_2O_3 compared to MPeA. Moreover, the complex prefers to form CD−MPeA = 1:1 structure either in solution or adsorbed on surface, probably due to H-bonding between "O—H---O" and "N---H—O", respectively. This type of interaction is not affected by the adsorption sequence of two species. Such behavior could possibly explain the fixed raised preferential enantioselectivity in this aliphatic alkenoic acid−cinchonidine system. The current work elucidates the intermolecular interactions of the acid−modifier complex in solution and at the metal oxide surface. Future work will focus on coupling these in situ spectroscopic measurements with kinetic investigations, aiming to understand the reaction mechanism of asymmetric C═C hydrogenation over cinchona-modified Pd.

ASSOCIATED CONTENT

Supporting Information

Details on the curve-fitting procedure for vibrational spectra are provided. This material is available free of charge via the Internet at http://pubs.acs.org.

AUTHOR INFORMATION

Corresponding Author

*E-mail: willia84@cec.sc.edu. Fax: (803)777-8265. Tel.: 803-777-0143.

Notes

The authors declare no competing financial interest.

ACKNOWLEDGMENTS

The authors gratefully acknowledge the financial support from National Science Foundation (CBET-0731074).

REFERENCES

(1) Tombo, G. M. R.; Bellus, D. Chirality and Crop Protection. *Angew. Chem., Int. Ed.* **1991**, *30* (10), 1193−1215.
(2) Collins, A. N.; Sheldrake, C. N.; Crosby, J., *Chirality in Industry: The Commercial Manufacture and Applications of Optically Active Compounds*. John Wiley & Sons: Chichester, UK, 1992; Vol. *1*.
(3) Noyori, R. Asymmetric Catalysis: Science and Opportunities (Nobel Lecture). *Angew. Chem., Int. Ed.* **2002**, *41* (12), 2008−2022.
(4) Sharpless, K. B. Searching for New Reactivity (Nobel Lecture). *Angew. Chem., Int. Ed.* **2002**, *41* (12), 2024−2032.
(5) Izumi, Y.; Imaida, M.; Fukawa, H.; Akabori, S. Asymmetric Hydrogenation with Modified Raney Nickel 0.1. Studies on Modified Hydrogenation Catalyst 0.2. *Bull. Chem. Soc. Jpn.* **1963**, *36* (1), 21−25.
(6) Sugimura, T.; Nakagawa, S.; Tai, A. Over 98% Optical Yield Achieved by a Heterogeneous Catalysis. Substrate Design and Analysis of Enantio-differentiating Factors of Tartaric Acid-modified Raney Nickel Hydrogenation. *Bull. Chem. Soc. Jpn.* **2002**, *75* (2), 355−363.
(7) Sugimura, T.; Osawa, T.; Nakagawa, S.; Harada, T.; Tai, A., *Stereochemical Studies of the Enantio-differentiating Hydrogenation of Various Prochiral Ketones over Tartaric Acid-modified Nickel Catalyst*; Elsevier Science Publishers B V: Amsterdam, 1996; Vol. *101*, pp 231−240.
(8) Orito, Y.; Imai, S.; Niwa, S. Asymmetric Hydrogenation of Methyl Pyruvate Using Pt-C Catalyst Modified with Cinchonidine. *Nippon Kagaku Kaishi* **1979**, *8*, 1118−1120.
(9) Mallat, T.; Orglmeister, E.; Baiker, A. Asymmetric Catalysis at Chiral Metal Surfaces. *Chem. Rev.* **2007**, *107* (11), 4863−4890.
(10) Blaser, H. U.; Studer, M. Cinchona-Modified Platinum Catalysts: From Ligand Acceleration to Technical Processes. *Acc. Chem. Res.* **2007**, *40* (12), 1348−1356.

(11) Borszeky, K.; Mallat, T.; Baiker, A. Enantioselective Hydrogenation of 2-Methyl-2-Pentenoic Acid over Cinchonidine-modified Pd/Alumina. *Catal. Lett.* **1996**, *41* (3−4), 199−202.
(12) Perez, J. R. G.; Malthete, J.; Jacques, J. Asymmetric Hydrogenation of Prochiral Cinnamic-Acids in the Presence of Palladium on Activated Carbon and of Chiral Bases. *Cr. Acad. Sci. II* **1985**, *300* (5), 169−172.
(13) Blaser, H. U. Enantioselective Synthesis Using Chiral Heterogeneous Catalysts. *Tetrahedron-Asymmetry* **1991**, *2* (9), 843−866.
(14) Bartok, M.; Wittmann, G.; Gondos, G.; Smith, G. V. Homogeneous and Heterogeneous Catalytic Asymmetric Reactions. 1. Asymmetric Hydrogenation of the Prochiral Carbon-Carbon Double Bond on a Modified Raney Nickel Catalyst. *J. Org. Chem.* **1987**, *52* (6), 1139−1141.
(15) Tan, S.; Monnier, J. R.; Williams, C. T. Kinetic Study of Asymmetric Hydrogenation of α, β-Unsaturated Carboxylic Acid Over Cinchona-Modified Pd/Al_2O_3 Catalyst. *Top. Catal.* **2012**, *55* (7), 512−517.
(16) Schurch, M.; Kunzle, N.; Mallat, T.; Baiker, A. Enantioselective Hydrogenation of Ketopantolactone: Effect of Stereospecific Product Crystallization During Reaction. *J. Catal.* **1998**, *176* (2), 569−571.
(17) Schurch, M.; Schwalm, O.; Mallat, T.; Weber, J.; Baiker, A. Enantioselective Hydrogenation of Ketopantolactone. *J. Catal.* **1997**, *169* (1), 275−286.
(18) Burgi, T.; Baiker, A. Conformational Behavior of Cinchonidine in Different Solvents: A Combined NMR and Ab initio Investigation. *J. Am. Chem. Soc.* **1998**, *120* (49), 12920−12926.
(19) Olsen, R. A.; Borchardt, D.; Mink, L.; Agarwal, A.; Mueller, L. J.; Zaera, F. Effect of Protonation on the Conformation of Cinchonidine. *J. Am. Chem. Soc.* **2006**, *128* (49), 15594−15595.
(20) Bartok, M.; Felfoldi, K.; Torok, B.; Bartok, T. A New Cinchona-modified Platinum Catalyst for the Enantioselective Hydrogenation of Pyruvate: the Structure of the 1: 1 Alkaloid-Reactant Complex. *Chem. Commun.* **1998**, *23*, 2605−2606.
(21) Bartok, M.; Sutyinszki, M.; Felfoldi, K.; Szollosi, G. Unexpected Change of the Sense of the Enantioselective Hydrogenation of Ethyl Pyruvate Catalyzed by a Pt-Alumina-Cinchona Alkaloid System. *Chem. Commun.* **2002**, *10*, 1130−1131.
(22) Carley, A. F.; Rajumon, M. K.; Roberts, M. W.; Wells, P. B. XPS and LEED Studies of 10,11-Dihydrocinchonidine Adsorption at Pt(111) - Implications for the Role of Cinchona Alkaloids in Enantioselective Hydrogenation. *J. Chem. Soc., Faraday Trans.* **1995**, *91* (14), 2167−2172.
(23) Simons, K. E.; Meheux, P. A.; Griffiths, S. P.; Sutherland, I. M.; Johnston, P.; Wells, P. B.; Carley, A. F.; Rajumon, M. K.; Roberts, M. W.; Ibbotson, A. A Model for the Enantioselective Hydrogenation of Pyruvate Catalyzed by Alkaloid-Modified Platinum. *Recl. Trav. Chim. Pays-Bas* **1994**, *113* (10), 465−474.
(24) Bond, G.; Wells, P. B. Enantioselective Hydrogenation 0.4. Hydrogen Isotope-Exchange in 10,11-Dihydrocinchonidine and in Quinoline Catalyzed by Platinum-Group Metals. *J. Catal.* **1994**, *150* (2), 329−334.
(25) Bartok, M.; Sutyinszki, M.; Balazsik, K.; Szollosi, G. Enantioselective Hydrogenation of Ethyl Pyruvate Catalysed by Cinchonine-modified Pt/Al_2O_3: Tilted Adsorption Geometry of Cinchonine. *Catal. Lett.* **2005**, *100* (3−4), 161−167.
(26) Evans, T.; Woodhead, A. P.; Gutierrez-Sosa, A.; Thornton, G.; Hall, T. J.; Davis, A. A.; Young, N. A.; Wells, P. B.; Oldman, R. J.; Plashkevych, O.; et al. Orientation of 10,11-Dihydrocinchonidine on Pt(111). *Surf. Sci.* **1999**, *436* (1−3), L691−L696.
(27) Kubota, J.; Zaera, F. Adsorption Geometry of Modifiers as Key in Imparting Chirality to Platinum Catalysts. *J. Am. Chem. Soc.* **2001**, *123* (44), 11115−11116.
(28) Ma, Z.; Zaera, F. Competitive Chemisorption Between Pairs of Cinchona Alkaloids and Related Compounds from Solution onto Platinum Surfaces. *J. Am. Chem. Soc.* **2006**, *128* (51), 16414−16415.
(29) Ferri, D.; Burgi, T.; Baiker, A. Chiral Modification of Platinum Catalysts by Cinchonidine Adsorption Studied by in situ ATR-IR Spectroscopy. *Chem. Commun.* **2001**, *13*, 1172−1173.
(30) Ferri, D.; Burgi, T.; Baiker, A. In situ ATR-IR Study of the Adsorption of Cinchonidine on Pd/Al_2O_3: Differences and Similarities with Adsorption on Pt/Al_2O_3. *J. Catal.* **2002**, *210* (1), 160−170.
(31) Cortes-Concepcion, J. A.; Williams, C. T.; Amiridis, M. D. ATR-IR Study of the Adsorption of 2 ′-Hydroxyacetophenone and Benzaldehyde on MgO. *Catal. Commun.* **2011**, *16* (1), 198−204.
(32) Tan, S.; Sun, X. J.; Williams, C. T. In situ ATR-IR Study of Prochiral 2-Methyl-2-Pentenoic Acid Adsorption on Al_2O_3 and Pd/Al_2O_3. *Phys. Chem. Chem. Phys.* **2011**, *13* (43), 19573−19579.
(33) Sun, X. J.; Williams, C. T. In-situ ATR-IR Investigation of Methylcinnamic Acid Adsorption and Hydrogenation on Pd/Al_2O_3. *Catal. Commun.* **2012**, *17*, 13−17.
(34) Schmidt, E.; Mallat, T.; Baiker, A. Substrate-controlled Adsorption of Cinchonidine During Enantioselective Hydrogenation on Platinum. *J. Catal.* **2010**, *272* (1), 140−150.
(35) Bonalumi, N.; Burgi, T.; Baiker, A. Interaction Between Ketopantolactone and Chirally Modified Pt Investigated by Attenuated Total Reflection IR Concentration Modulation Spectroscopy. *J. Am. Chem. Soc.* **2003**, *125* (44), 13342−13343.
(36) Meemken, F.; Maeda, N.; Hungerbühler, K.; Baiker, A. Platinum-Catalyzed Asymmetric Hydrogenation: Spectroscopic Evidence for an O-H-O Hydrogen-Bond Interaction Between Substrate and Modifier. *Angew. Chem., Int. Ed.* **2012**, *51* (33), 8212−8216.
(37) Meier, D. M.; Urakawa, A.; Turra, N.; Ruegger, H.; Baiker, A. Hydrogen-bonding Interactions in Cinchonidine-2-Methyl-2-Hexenoic Acid Complexes: A Combined Spectroscopic and Theoretical Study. *J. Phys. Chem. A* **2008**, *112* (27), 6150−6158.
(38) Ortiz-Hernandez, I.; Williams, C. T. In Situ Investigation of Solid-Liquid Catalytic Interfaces by Attenuated Total Reflection Infrared Spectroscopy. *Langmuir* **2003**, *19* (7), 2956−2962.
(39) Chu, W.; LeBlanc, R. J.; Williams, C. T.; Kubota, J.; Zaera, F. Vibrational Band Assignments for the Chiral Modifier Cinchonidine: Implications for Surface Studies. *J. Phys. Chem. B* **2003**, *107* (51), 14365−14373.
(40) Busygin, I.; Tkachenko, O. P.; Nieminen, V.; Sillanpää, R.; Toukoniitty, E.; Kustov, L. M.; Murzin, D. Y.; Leino, R. Interaction of Cinchonidine and 1-Phenyl-1,2-Propanedione on the Surface of a Chirally Modified Pt/Al_2O_3 Hydrogenation Catalyst. *J. Phys. Chem. C* **2007**, *111* (26), 9374−9383.
(41) Ferri, D.; Burgi, T. An in situ Attenuated Total Reflection Infrared Study of a Chiral Catalytic Solid-Liquid Interface: Cinchonidine Adsorption on Pt. *J. Am. Chem. Soc.* **2001**, *123* (48), 12074−12084.
(42) Liu, Z.; Li, X.; Ying, P.; Feng, Z.; Li, C. Fourier Transform Infrared Spectroscopic Study on the Adsorption of Ethyl Pyruvate on Pt/Al_2O_3: Side Reactions Suppressed by Adsorbed Hydrogen and Cinchonidine. *J. Phys. Chem. C* **2006**, *111* (2), 823−829.
(43) Greenler, R. G.; Snider, D. R.; Witt, D.; Sorbello, R. S. The Metal-Surface Selection Rule for Infrared-Spectra of Molecules Adsorbed on Small Metal Particles. *Surf. Sci.* **1982**, *118* (3), 415−428.
(44) Ma, Z.; Zaera, F. Role of the Solvent in the Adsorption-Desorption Equilibrium of Cinchona Alkaloids Between Solution and a Platinum Surface: Correlations Among Solvent Polarity, Cinchona Solubility, and Catalytic Performance. *J. Phys. Chem. B* **2005**, *109* (1), 406−414.
(45) Ferri, D.; Burgi, T.; Baiker, A. FTIR Study of Chiral Modifier-Reactant Interactions. The Cinchonidine-Alkenoic Acid System. *J. Chem. Soc., Perkin Trans. 2* **2002**, No. 3, 437−441.
(46) Bisignani, R.; Franceschini, S.; Piccolo, O.; Vaccari, A. The Solvent Effect in the Enantioselective Hydrogenation of (E)-2-Methyl-2-Butenoic Acid with Cinchonidine Doped Pd/Al_2O_3. *J. Mol. Catal. A: Chem.* **2005**, *232* (1−2), 161−164.
(47) Nitta, Y.; Shibata, A. Enantioselective Hydrogenation of (E)-alpha-Phenylcinnamic Acid on Pd/TiO_2 Catalyst Modified by Cinchona Alkaloids: Effect of Modifier Structure. *Chem. Lett.* **1998**, No. 2, 161−162.

(48) Kun, I.; Torok, B.; Felfoldi, K.; Bartok, M. Heterogeneous Asymmetric Reactions Part 17. Asymmetric Hydrogenation of 2-Methyl-2-Pentenoic Acid over Cinchona Modified Pd/Al_2O_3 Catalysts. *Appl. Catal. A: Gen.* **2000**, *203* (1), 71−79.
(49) Szollosi, G.; Balazsik, K.; Bartok, M. Enantioselective Hydrogenation of Itaconic Acid over Cinchona Alkaloid Modified Supported Palladium Catalyst. *Appl. Catal. A: Gen.* **2007**, *319*, 193−201.
(50) Szollosi, G.; Herman, B.; Fulop, F.; Bartok, M. Cinchona Methyl Ethers as Modifiers in the Enantioselective Hydrogenation of (E)-2,3-Diphenylpropenoic Acids over Pd Catalyst. *J. Catal.* **2010**, *276* (2), 259−267.
(51) Szollosi, G.; Busygin, I.; Herman, B.; Leino, R.; Bucsi, I.; Murzin, D. Y.; Fulop, F.; Bartok, M. Inversion of the Enantioselectivity in the Hydrogenation of (E)-2, 3-Diphenylpropenoic Acids over Pd Modified by Cinchonidine Silyl Ethers. *ACS Catal.* **2011**, *1* (10), 1316−1326.
(52) Szollosi, G.; Niwa, S. I.; Hanaoka, T. A.; Mizukami, F. Enantioselective Hydrogenation of alpha,beta-Unsaturated Carboxylic Acids over Cinchonidine-modified Pd Catalysts: Effect of Substrate Structure on the Adsorption Mode. *J. Mol. Catal. A: Chem.* **2005**, *230* (1−2), 91−95.
(53) Schmidt, E.; Bucher, C.; Santarossa, G.; Mallat, T.; Gilmour, R.; Baiker, A. Fundamental Insights into the Enantioselectivity of Hydrogenations on Cinchona-modified Platinum and Palladium. *J. Catal.* **2012**, *289*, 238−248.